Astron. Astrophys. 325, 551–558 (1997)

ASTRONOMY
AND
ASTROPHYSICS

Detection of planetary spectral features of extrasolar planets through their circumstellar dust – a Monte Carlo simulation

O. Fischer and W. Pfau

Astrophysikalisches Institut und Universitäts-Sternwarte, Schillergäßchen 2, D-07745 Jena, Germany

Received 10 December 1996 / Accepted 21 March 1997

Abstract. One of the methods envisaged to detect planets outside of our solar system assumes that certain spectral features at 10 and below 20 μm wavelength are typical of planetary atmospheres. Their detection would then be an unambiguous sign of the presence of extrasolar planets. In these spectral regions, there might be interference with the silicate and ice features of circumstellar material still associated with the system. In order to get an estimate of this effect, we used our 3D Monte Carlo radiation transport code to model the spectrum of a Keplerian disk with embedded artificial planets encircling a central star of solar luminosity and temperature. The disk structure and the grain model resemble real properties in protoplanetary disks, the temperature distribution was calculated independently. Three models with different circumstellar dust populations and disk structure were calculated, each of them for two debris disk masses. From the observational point of view, various beam sizes and positions of the observer in respect to the configuration were taken into account. The detectability of the embedded planetary sources is discussed. The results show strong constraints on the detection of planetary atmospheric features through circumstellar dust.

Key words: radiative transfer – methods: statistical – interplanetary medium – planets and satellites: general – stars: circumstellar matter – stars: planetary systems – infrared: solar system

1. Introduction

The detection of extra-solar planetary systems is one of the great challenges to contemporary astronomy. Adapted to the ambitious task, practically all the main observational techniques seem in principle to be capable to contribute to the aim. Different planet-detection techniques have however different "discovery spaces" which define the subsets of extrasolar planets with the best chances of discovery. Observations from the ground and from space, even from the stratosphere were proposed. The status of proposals and methods as of the end of 1992 was summarized in the proceedings of the conference on *Planetary Systems: Formation, Evolution, and Detection* (Burke et al. 1994). Recent reports on the subject were given by Schneider (1996 a, b), e.g. .

The proposals refer to a broad wavelength range from optical and infrared to millimetre bands. In cases were the planetary body itself is to be observed, the contrast to the parent star is smaller at longer wavelengths.

Direct *imaging* using sophisticated coronographic apodization methods, high-resolution IR arrays, speckle methods, and aperture synthesis in the radio region aim to unveil planet-like companions close to carefully selected target stars. Other methods are directed to measure and model the morphology and physical parameters of circumstellar structures related to planetary systems in their earliest phases. Eclipsing binaries offer the chance that the lines of sight are sufficiently close to the orbital plane of the suspected planets. The transits of inner planetary bodies might be detected from *monitoring photometry* as a measurable modulation of the stellar light. Doyle et al. (1996) reported on a dozen candidate transit events in the CM Dra system, observed within their Transit of Extrasolar Planets programme. A very promising search technique is offered by *gravitational lensing*. Planets (down to 10^{-6} $M_\odot$) passing near the line of sight to distant stars will cause a brief brightening of the stellar light. Further potentials are in the *spectrophotometry*. Respective methods aim at the detection of characteristic atmospheric bands, the A band of O_2 at 760 nm and the O_3 band at 9.6 μm, e.g. In principle one can try to observe the bands directly in the planet's spectrum separated from the stellar one, or as a transient phenomenon in the stellar spectrum when the planet occults the star and stellar radiation traces the planetary atmosphere. The most promising and meanwhile successful methods are given by *accelerometry* and *astrometry* . These indirect methods are making use of the gravitational interaction between the central star and its companion(s), which causes a motion of the components around the common barycentre. This should be reflected in a varying radial velocity and a positional variation of the observable star. In the past, periodic terms in the proper motion were

Send offprint requests to: O. Fischer, fischer@astro.uni-jena.de

observed for several stars, but the accuracy of classical methods is not sufficient to detect companions of planet-like masses. Here interferometric methods are demanded. High-resolution spectroscopy was successful, however, to definitely detect companions of masses of the order of the Jupiter mass in the case of a few nearby stars (Mayor & Queloz 1995). Orbital motion is responsible for the characteristic pattern in the arrival times of pulses from the PSR 1257+12 pulsar observed by Wolszczan & Frail (1992) as well as for the drift in the timing of eclipsing binaries (see Doyle et al. 1996).

This paper is concerned with the detection of spectroscopic features assumed to be typical of the atmospheres of Earth- and Jupiter-like planets in general. Especially in the infrared spectral region with the enhanced contrast to the emission of the central star, this might be a powerful tool to detect extrasolar planets. IR spectra of solar system planets (see Burke 1992) show prominent absorption and emission features due to atmospheric constituents. Besides pointing to the existence of an atmosphere, these features could help to find out whether atmospheres of extrasolar planets can be classified as CO_2- or CH_4-dominant ones, as it is the case with Earth- and Jupiter-like planets, resp. The detection of ozone would be a strong indicator of Earth-like biological activity. Methane in coexistence with ozone would give us an additional argument for life as a "chemical reactor". Without biological activity methane would be oxidized and thus disappear.

Even in relatively late phases when planet-like bodies have already formed, the disk structure surrounding a star may still contain such an amount of diffuse material that the detection of certain atmospheric features of the extrasolar planet is severely hampered. The features might be washed out by emission from circumstellar material or are hidden in the noise from radiation scattered or reemitted by circumstellar dust particles along the line of sight to the planets. To evaluate the amount of dust which does not significantly influence the atmospheric bands, Monte Carlo simulations of radiative transfer were performed in configurations consisting of an Earth- and a Jupiter-like planet embedded in a debris dust disk around a solar-type central star. We restricted our investigation to the O_3 ν_1 and ν_3 bands at λ = 9.6 μm and the CO_2 ν_2 band at λ = 15.0 μm (see Fig 3), which interfere with circumstellar silicate and methanol features at λ = 10 μm and 18 μm. The calculations were done for two different grain models, total dust masses and for different viewing angles. In one of the models the presence of gaps in the disk due to perturbations from the orbiting planets is assumed.

In Sect. 2 the physical properties of our models are described and the results are presented and discussed in Sects. 3 and 4, resp.

2. Modelling

The model configurations for an extrasolar system were assumed in imitation of our solar system - with a solar-like central star ($T_{\rm eff}$ = 5870 K, $R_\odot \approx 7 \cdot 10^8$ m) and two planets at distances and with emissions like Earth and Jupiter (planetary photon fluxes were taken from Burke (1992, p. 78). Star and planets are embedded in a circumstellar dust disk which represents the remnant material from planet formation.

2.1. Circumstellar dust

Assumptions about the properties and the distribution of the circumstellar dust and the temperature distribution in the debris disk are mainly made on the basis of observational hints from Vega phenomenon dust as it was detected around α Lyr, α PsA, and, as a particularly clear case, for β Pic.

2.1.1. Debris dust disk

The dust was modelled as orbiting about the central star in a Keplerian disk. The density distribution of such a disk is given by (Shakura & Sunyaev 1973):

$$\rho(r,z) = \rho_{\rm D} \left(\frac{r}{r_{\rm D}}\right)^{-1.875} \exp\left(\frac{-\pi}{4}(\frac{z}{h(r)})^2\right),$$

with

$$h(r) = z_{\rm D} \left(\frac{r}{r_{\rm D}}\right)^{1.125}.$$

For the disk parameters we used radius $r_{\rm D}$ = 100 AU, thickness $z_{\rm D}$ = 10 AU, and the midplane density in the range of $\rho_{\rm D} = 10^{-18} \ldots 10^{-19}$ g/cm^3.

Ground based and IUE spectroscopic studies (Lagrange-Henri et al. 1989) of the β Pic debris disk have provided hints at the precense of a central hole and gaps. We assumed the inner edge of the disk to be at a radius of 0.25 AU. Gaps in the disk along the orbits of the planets are introduced in our third model. The width of these gaps was taken from the relation

$$\Delta a_{\rm planet} \approx 1.5\ a_{\rm planet} \cdot \mu^{2/7} \quad (1)$$

which predicts the onset of chaotic behaviour of a test particle in the planar and circular restricted three-body problem inside the semimajor axis region $a_{\rm planet} \pm \Delta a_{\rm planet}$ (see Duncan et al. 1989, Holman & Wisdom 1993). The quantity μ is the ratio of the masses of the planet and the Sun. From (1) we got gaps in the disk at $a \approx (1.00 \pm 0.04)$ AU for the Earth and $a \approx (5.20 \pm 1.07)$ AU for Jupiter.

The total disk masses assumed in our models are in the range of $10^{-8} \ldots 10^{-7}$ M$_\odot$ (for a gas/dust ratio of 100, dust masses are in the range of about $3 \cdot 10^{-5} \ldots 3 \cdot 10^{-4}$ M$_\oplus$), corresponding to masses possible for debris disks around G-type main-sequence stars (André 1994). The midplane density of the solar system interplanetary dust of $\approx 10^{-19}$ kg/m^3 at 1 AU (Leinert & Grün 1990) is about $10^2 \ldots 10^3$ times lower than in our less evolved debris disk.

Because each run of the Monte Carlo simulation of the radiative transfer is done for only one wavelength, we need an approximation of the temperature distribution in the disk. As a first attempt we modelled the emission from the mid-size grains by $T \propto r^{-0.4}$ (Artymowicz et al. 1989). For a distance of 1 AU we took T = 150 K.

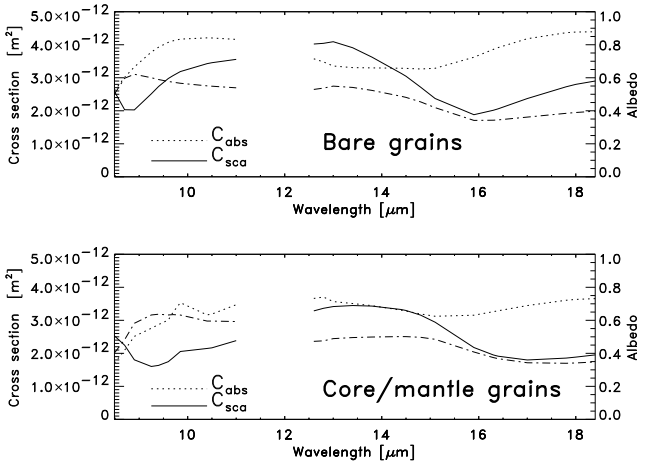

Fig. 1. Cross sections (absorption, scattering) and albedos for the two different populations of circumstellar dust. The bare grains consist of 60 % olivines and 40 % pyroxenes with radii $a = 0.1 \ldots 10.0 \mu$m ($n(a) \propto a^{-2}$). The core/mantle grains are made of bare grain material in the core and the weak interstellar mix (H_2O:CH_3OH:CO:NH_3 = 100:10:1:1, Hudgins et al. 1993) in the mantle. The core radii are $a = 0.079 \ldots 7.94 \mu$m, the core+mantle radii $a = 0.1 \ldots 10.0 \mu$m, ($n(a) \propto a^{-2}$).

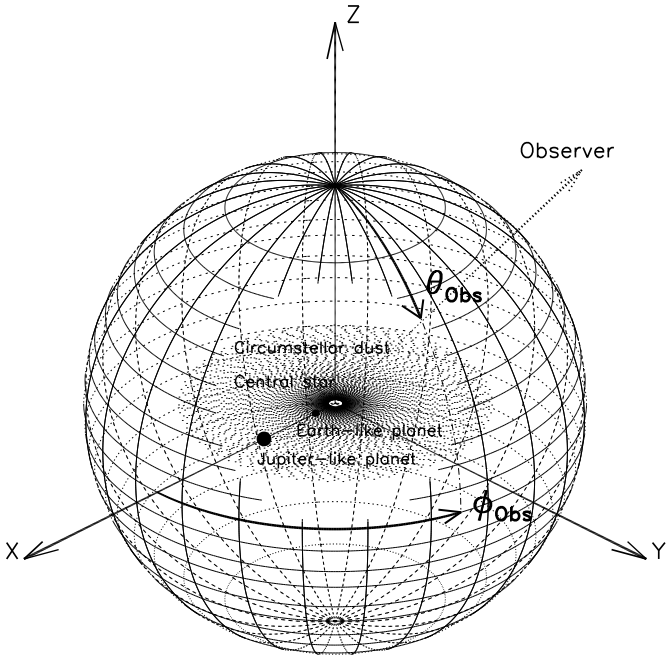

Fig. 2. Geometry of the 3D radiative tranfer model.

2.1.2. Dust properties

The β Pic spectrum indicates the existence of micron-sized silicate particles (Knacke et al. 1993). For the dust population in our debris disk model we used grains with radii $a = 0.1 \ldots 10$ μm and a distribution $n(a) \propto a^{-2}$. For the dust composition we applied the main components of the interplanetary dust particle (IDP) population proposed by Sandford (1988), which give quit well a fit to the β Pic spectrum – 60% olivines ($MgFeSiO_4$) and 40% pyroxenes ($Mg_{0.8}Fe_{0.2}$ SiO_3). The optical constants for the bare silicate grains are taken from Dorschner et al. (1995) who prepared silicate glasses as laboratory analogues of circumstellar silicate dust.

In a second model variant we introduced an ice component to the dust in form of a mantle. For the core/mantle grains we assumed a mantle-to-core volume ratio V_m/V_c of 1 which lies in the range of values found on the line of sight to the Becklin-Neubebauer object (Lee & Draine 1985). On the basis of V_m/V_c and outer (core+mantle) grain radii of $a = 0.1 \ldots 10$ μm we deduced core radii of $a = 0.079 \ldots 7.94$ μm. The functional dependence of the grain size distribution is the same as for the population of bare grains. For the grain cores we used the bare grain dust. For the ice mantles mixed molecular ices were applied. Hudgins et al. (1993) calculated the optical constants for a variety of pure and mixed molecular ices. From their data we selected the so-called weak interstellar mix (H_2O:CH_3OH:CO:NH_3 = 100:10:1:1) at a medium temperature of 80 K (Hudgins et al. 1993, Table 2C).

2.2. Monte Carlo simulation of radiative transfer

For our investigation we performed monochromatic radiative transfer calculations at 11 wavelength points in the range $\lambda = 8.5 \ldots 11.0$ μm for the O_3 band and at 16 wavelength points in the range $\lambda = 12.6 \ldots 18.4$ μm for the CO_2 band.

The principal task of the Monte Carlo simulation of radiative transfer is to construct a stochastic model in which the expected values of the intensities have to be determined. This model consists of the random walk of a weighted photon. The random path is determined by the random quantities: starting-point, free path lengths and propagation directions. We started weighted photons from four sources: the central star, the two planets, and the thermally emitting dust (photon fluxes of the sources are shown in Fig. 3, luminosity ratios star/planet and disk/planet are given for $\lambda = 9.85$ and 15.1 μm in Table 1). During the course of the random walk of a weighted photon, the initial intensity (weight) will be changed as the result of scattering events and absorption. After the last scattering (or without any scattering event), the weighted photon becomes "observable". In our 3D-model (Fig. 2), we can "observe" the configuration from 480 positions around it. Therefore, the full solid angle of all possible observer directions is divided into 480 equal sized solid angle intervalls of $\pi/120$. The centre of each intervall is determined by the angles θ_{obs} und ϕ_{obs}. The photons are accumulated in circles of different size (0.173 . . . 1.73 AU in diameter) centred on the lines of sight to the planets (comparable with beam sizes).

The accuracy of the resulting intensities growths with increasing number N of weighted photons accumulated in the circles (error $\propto 1/\sqrt{N}$).

The large demand of computing time is an essential disadvantage of the Monte Carlo method. The computations were

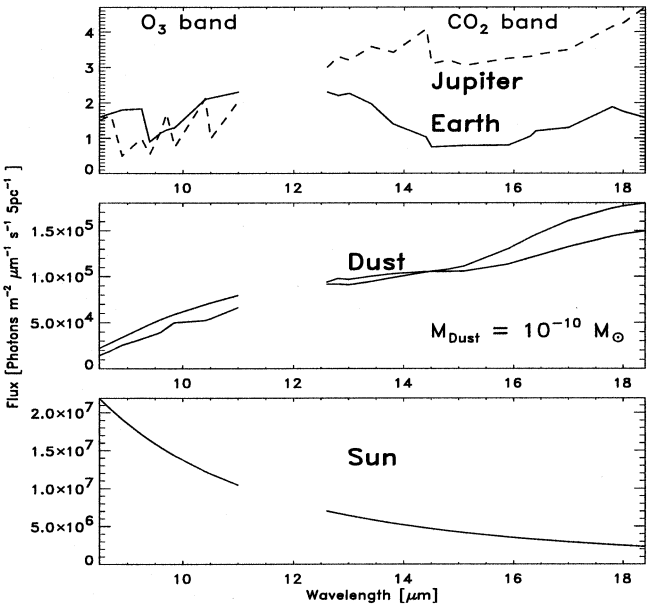

Fig. 3. Sources of emission in the model. The thermal dust emission is shown for both the circumstellar dust populations: bare silicate grains – upper curve, core+mantle grains – lower curve.

Table 1. Ratios of luminosities (star/planet, dust disk/planet). In case of the disk, three types, each with two densities were assumed in the modelling (see Sect. 2.1.1).

	9.85 μm	15.1 μm
$\frac{L_{\rm Star}}{L_{\rm Earth}}$	$1.1 \cdot 10^7$	$5.3 \cdot 10^6$
$\frac{L_{\rm Star}}{L_{\rm Jupiter}}$	$1.9 \cdot 10^7$	$1.4 \cdot 10^6$
$\frac{L_{\rm Dust}}{L_{\rm Earth}}$	$4.5/5.4/5.3 \cdot 10^4/10^5$	$1.4/1.9/1.8 \cdot 10^5/10^6$
$\frac{L_{\rm Dust}}{L_{\rm Jupiter}}$	$7.9/9.4/9.2 \cdot 10^4/10^5$	$3.6/5.0/4.7 \cdot 10^4/10^5$

performed on α-DEC-Workstations (200 series, 3000 series, SMP A2100/4). Dependent on the type, a CPU time of several hours was necessary for the transport of 10^7 weighted stellar photons per wavelength.

More details about the Monte Carlo simulation of radiative transfer can be found in Fischer et al. (1994) and Fischer (1995).

3. Results

Three circumstellar dust models were investigated (each for dust disk masses of $3 \cdot 10^{-5}$ and $3 \cdot 10^{-4}$ $M_\oplus$):

1.) with bare silicate grains, without gaps in the disk,
2.) with core/mantle grains, without gaps in the disk, and,
3.) with core/mantle grains and gaps in the disk.

We performed the radiative transfer separating the effects of scattered stellar radiation and the thermally emitted (and scattered) dust radiation from the planet radiation. The last one was taken without transfer because of the negligible changes expected in comparison to the effects mentioned before.

Three "observer's positions" between the pole-on and edge-on view and normally to the line connecting the central star with the planets (x-axis in our model) were selected.

Despite the large number of weighted photons started from the star ($2 \cdot 10^7$ for each wavelength), the statistical error is still large because of the very low probability of scattering in case of the debris disks used for the calculations. The error increases (as the number of collected weighted photons decreases) going from the Earth-like to the Jupiter-like planet, from edge-on to pole-on positions, and from large to small beam sizes. For the interpretation we have to take notice of this "noise effect".

The effects of the beam size and the position in respect to the disk are obvious (see Figs. 4, 5, 6). Close to the pole-on view no absorption acts and the curves for scattered stellar light show the distribution of $C_{\rm sca}$ (see Fig. 1). For higher inclination angles $\theta_{\rm obs}$ this light becomes increasingly absorbed. As a consequence the minimum in the $8.5 \cdots 9$ μm range is partly filled in and shifted to larger wavelengths. In case of the thermal dust contribution, the curves for the Earth are similiar to the curves for the emission from the whole dust. The course of the Jupiter curves differs especially in the O_3 band range.

The resulting scattered and reemitted photon portions are shown in Figs. 4 and 5 for a dust disk mass of $3 \cdot 10^{-5} M_\oplus$ and of $3 \cdot 10^{-4} M_\oplus$, respectivly. In Fig. 6 we summed up all photon portions to show the influence of the circumstellar dust radiation on the O_3 and CO_2 bands at different beam sizes.

4. Discussion and conclusions

Our results show that (as expected) the discovery of atmospheric bands of planets through circumstellar dust of a debris disk strongly depends on the dust mass, i. e. the age of the central star. Dust population and disk structure (gaps) also influence the probability of detection of planetary spectral features as well as their shape. From the observational point of view, beam size and the observer's position in respect to the disk determine the contrast of the band features to the spectral background.

- In all cases, a band detection is most likely for pole-on candidates. As a consequence, extra-solar planets candidates detected indirectly by astrometry (e. g., Lalande 21185, Walker 1996) are preferred objects which should be investigated for spectroscopic features.
- It is important to know what additional emission component from the debris disk influences the band features most – the thermal dust emission or scattering. For Earth-like planets photons from the thermal dust radiation dominate the whole wavelength range of investigation. Because of the increase of the number of thermal photons with wavelength, the O_3 ν_1 and ν_3 bands (9.6 μm) are easier to be detected than the CO_2 ν_2 band (15 μm).
  In case of Jupiter-like planets we can find more scattered stellar photons shortward of about 14 μm. Larger wavelengths are again dominated by thermal photons.

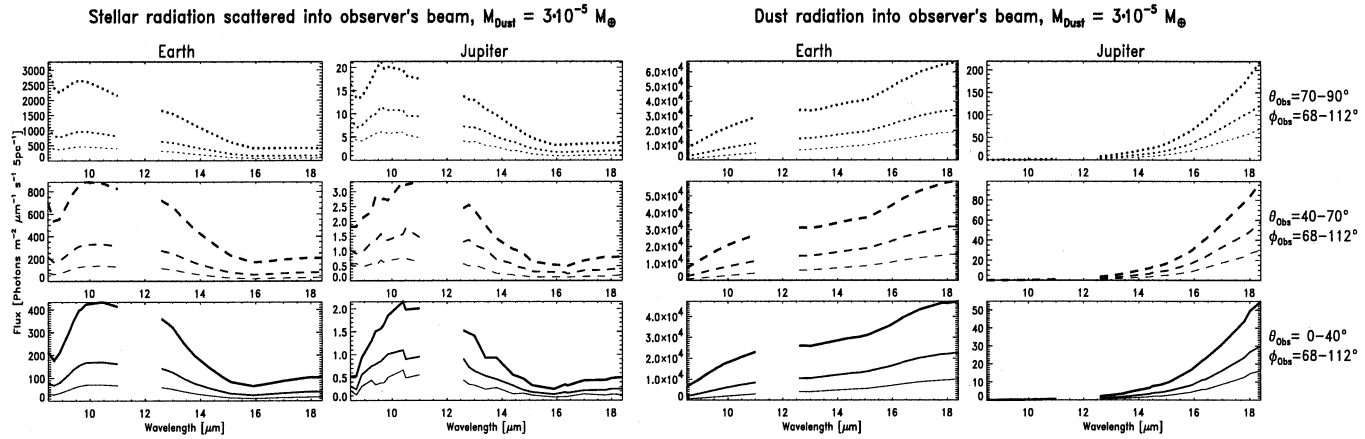

Model 1: Bare silicate grains, no gaps

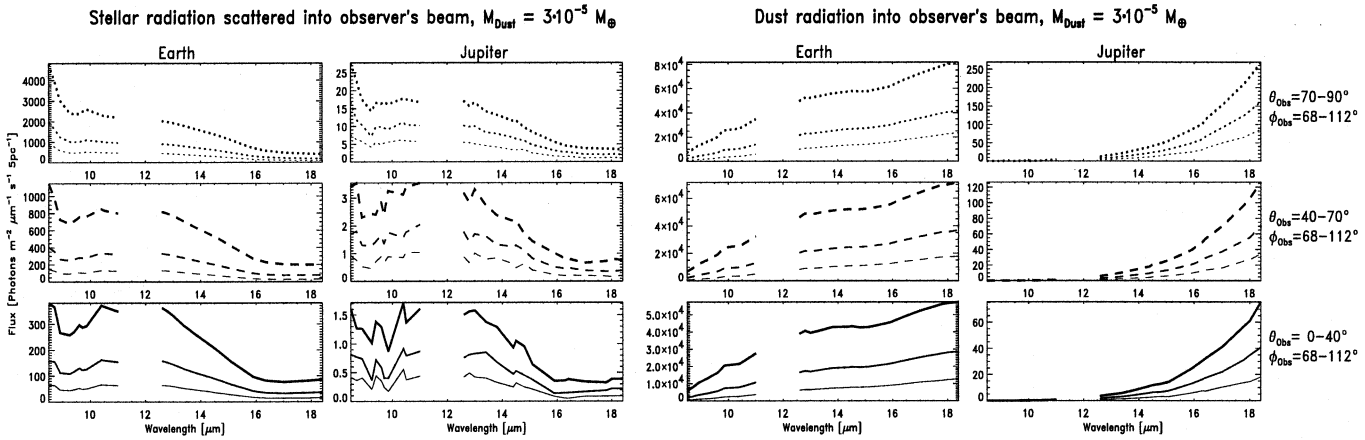

Model 2: Core-mantle grains, no gaps

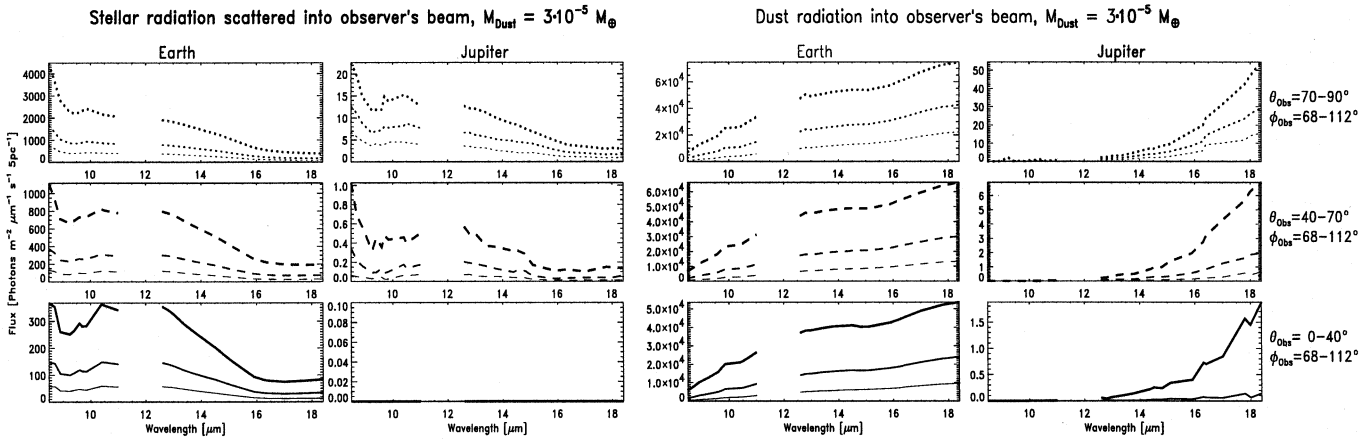

Model 3: Core-mantle grains, disk with gaps

Fig. 4. Photon fluxes of scattered stellar radiation and thermal dust radiation at a distance of 5 pc for different models with debris dust masses of $3 \cdot 10^{-5}$ $M_\oplus$. Beam sizes decrease with decreasing line thickness: 1.7, 1.3, 1.0 AU. Various "observer's positions" between the edge-on and pole-on view normally to the line connecting the central star with the planets are presented by various line styles: dotted lines: $\theta_{\rm obs} = 70 \ldots 90°$, $\phi_{\rm obs} = 68 \ldots 112°$, dashed lines: $\theta_{\rm obs} = 40 \ldots 70°$, $\phi_{\rm obs} = 68 \ldots 112°$, solid lines: $\theta_{\rm obs} = 0 \ldots 40°$, $\phi_{\rm obs} = 68 \ldots 112°$. To get a better statistics, we averaged the results within the angular ranges indicated.

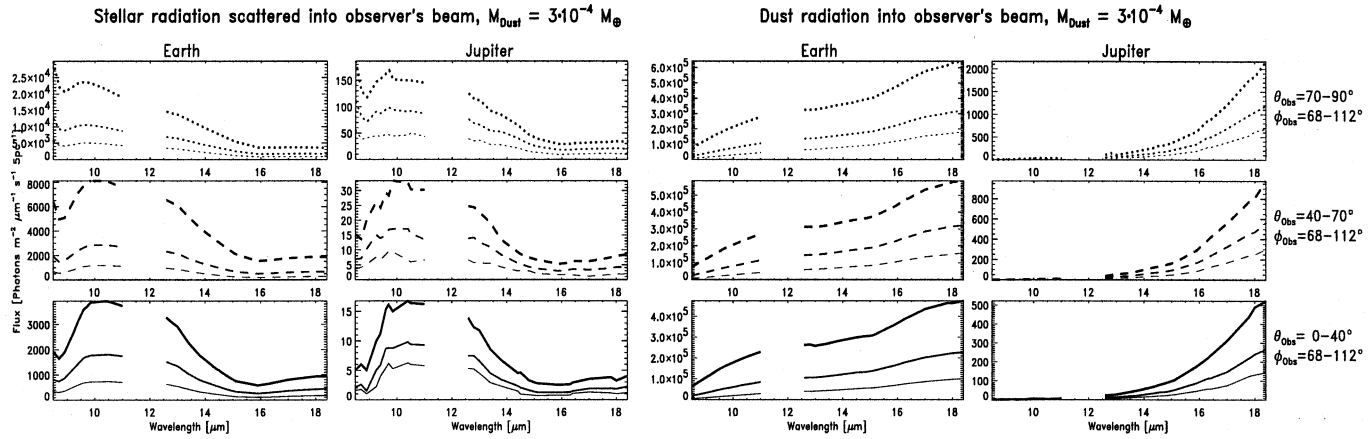

Model 1: Bare silicate grains, no gaps

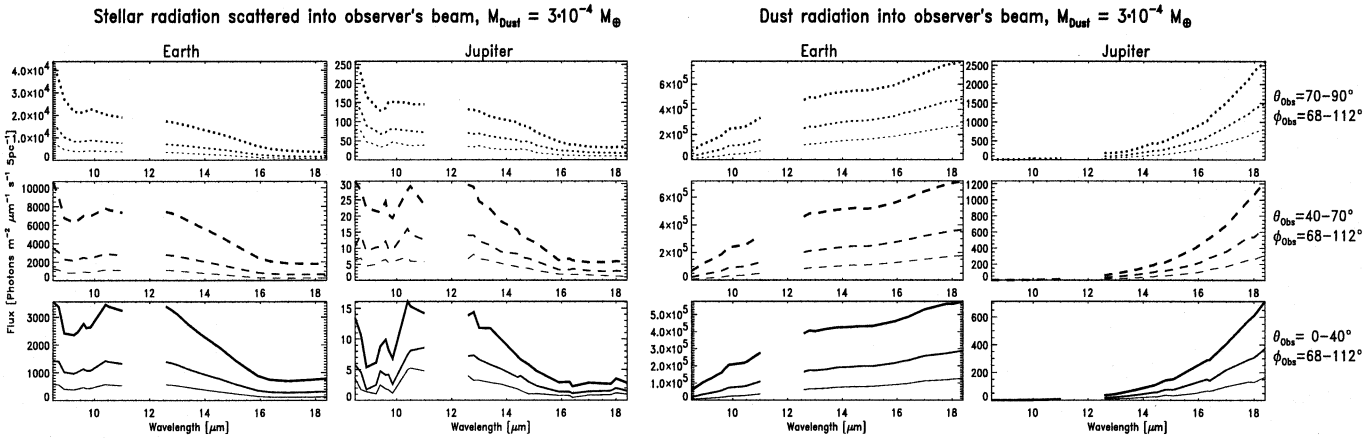

Model 2: Core-mantle grains, no gaps

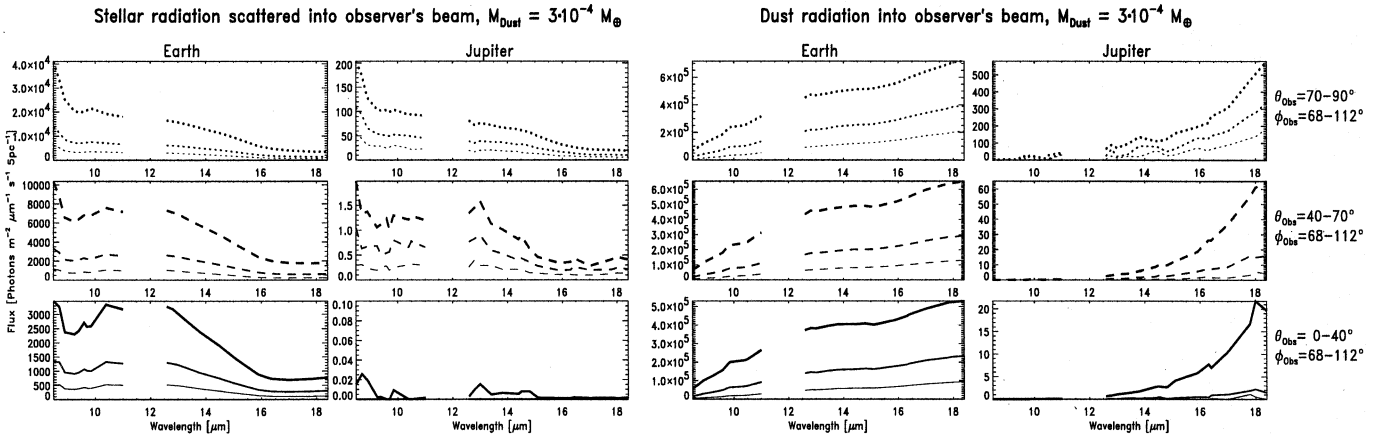

Model 3: Core-mantle grains, disk with gaps

Fig. 5. Photon fluxes of scattered stellar radiation and thermal dust radiation at a distance of 5 pc for different models with debris dust masses of $3 \cdot 10^{-4}$ $M_\oplus$.. Beam sizes decrease with decreasing line thickness: 1.7, 1.3, 1.0 AU. Various "observer's positions" between the edge-on and pole-on view normally to the line connecting the central star with the planets are presented by various line styles: dotted lines: $\theta_{\rm obs} = 70 \ldots 90°$, $\phi_{\rm obs} = 68 \ldots 112°$, dashed lines: $\theta_{\rm obs} = 40 \ldots 70°$, $\phi_{\rm obs} = 68 \ldots 112°$, solid lines: $\theta_{\rm obs} = 0 \ldots 40°$, $\phi_{\rm obs} = 68 \ldots 112°$. To get a better statistics, we averaged the results within the angular ranges indicated.

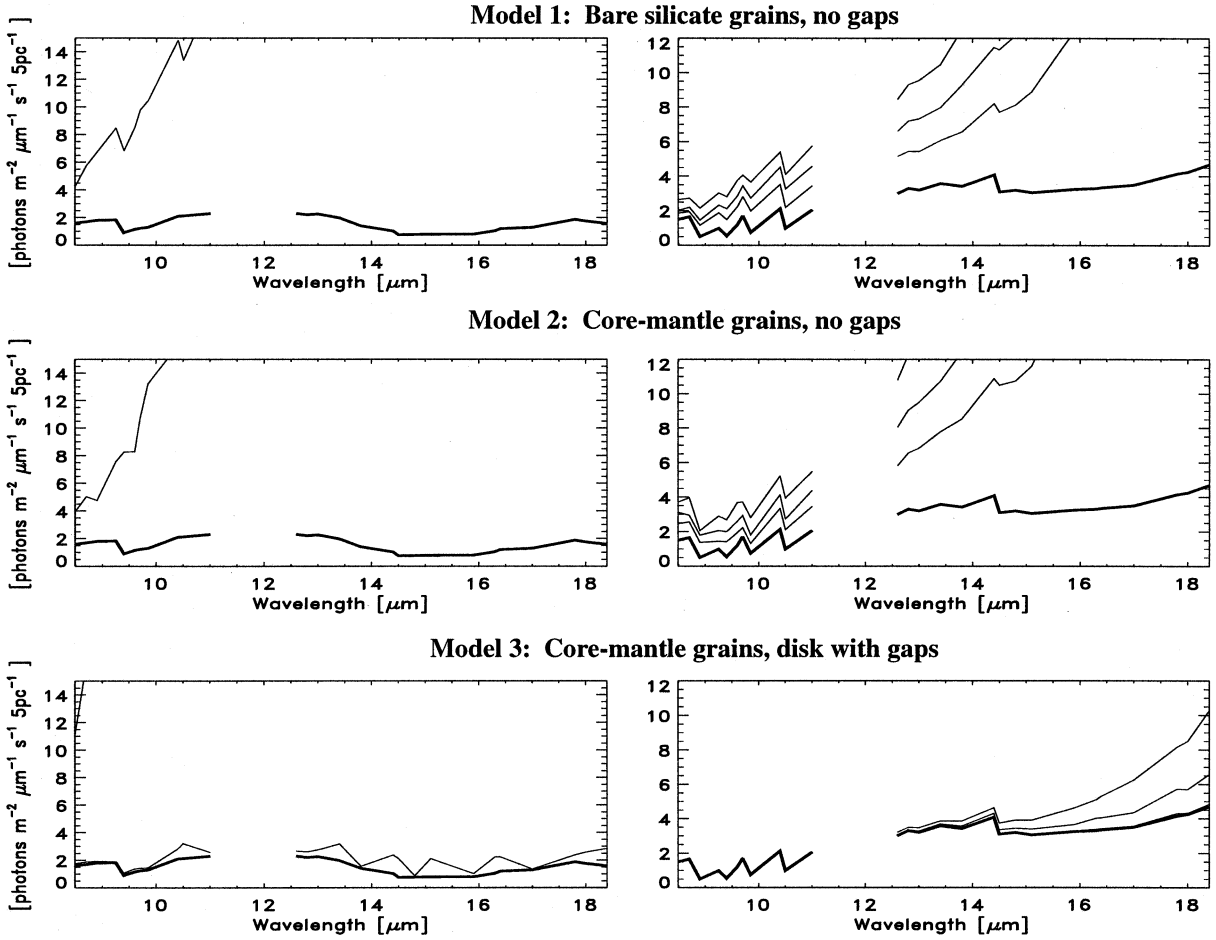

Fig. 6. Sum of all photon flux components, i. e., planet radiation + scattered stellar radiation + thermal dust radiation, in the observer's beam for the pole-on view onto the $3 \cdot 10^{-5}$ $M_\oplus$ dust disk. Beam sizes (diameters) correspond to linear disk dimensions of 0.09, 0.26, 0.43 AU for Earth-like and 1.1, 1.4, 1.7 AU for Jupiter-like planets (thin lines). The lowest (thick) line represents the planet radiation alone (see also Fig. 3). The graphs for the Earth-like planet show a large statistical noise because of the low number of photons collected (in the Monte Carlo calculation) with very small beam sizes.

- To get photon fluxes for the O_3 bands from an Earth-like planet comparable with the fluxes from the thermally emitting dust, beam sizes smaller than 0.1 AU are necessary for the $3 \cdot 10^{-5}$ $M_\oplus$ dust disk close to the pole-on view (for the disk with gaps see the following point). For the $3 \cdot 10^{-4}$ $M_\oplus$ dust disk the beam size has to be even smaller.
  In case of the Jupiter-like planet, beam sizes in the range of about 1 AU would allow to detect a CO_2 band within a $3 \cdot 10^{-5}$ $M_\oplus$ dust disk close to the pole-on view (see also the following point). For edge-on configurations, this beam size has to be reduced by half (a quarter in area). Going to the $3 \cdot 10^{-4}$ $M_\oplus$ dust disk, we need an about three times smaller beam size. Atmospheric features in the range of up to about 12 μm (possible features of CH_4-dominated atmospheres at shorter wavelengths: CH_4 ν_4 at 7.7 μm, C_2H_6 ν_9 at 12.2 μm) can be already detected with ≈ 1 AU beams for the $3 \cdot 10^{-4}$ $M_\oplus$ pole-on dust disk or at any tilt for the $3 \cdot 10^{-5}$ $M_\oplus$ dust disk.
- Gaps in the disk can significantly increase the detection probability of planetary spectral features for Jupiter-like planets near their pole-on view (see Fig. 6). In this case, the O_3 band of the Earth-like planet can be already discovered in the $3 \cdot 10^{-5}$ $M_\oplus$ disk using a 0.2 . . . 0.3 AU beam size. In case of the Jupiter-like planet a detection of atmospheric features seems to be possible with beam sizes of some AU.
- A method to get planet fluxes with larger beam sizes (still small enough to get well resolved disk images) could be their separation from the asymmetric disk image assuming central symmetry for the disk alone.
- By the aid of the "large beam size curves" in Figs. 4 and 5 which due to their lower statistical noise give an impression of the course of the photon fluxes with wavelength, we can derive how the band profiles change by the inference from the "background disk light".

So we predict that the long wavelength wing of the O_3 band is raised by the thermal dust emission continuum. The same effect is expected for Jupiter's spectral features around 15 μm (see Fig. 6). In case of core-mantle grains a thermal dust emission feature is expected short before 10 μm (see Fig. 1). This would lead to a bump in the ozone feature of the Earth-like planet.

The ozone band is also influenced by scattered light. Especially the ice feature of the core-mantle grains can be misinterpreted as O_3 band. Bands of Jupiter-like planets are changed by scattered light up to about 12 μm. A strong influence is expected for the CH_4 ν_4 band at 7.7 μm.

- Taking into account a correlation between the age of the central star and the circumstellar dust mass (André 1994, t^{-2} variation), Jupiter-like planets should be detectable by their spectral characteristics up to about $\lambda = 15$ μm using beam sizes < 1 AU around G-type stars with ages larger than 10^9 yr. Earth-like planets can be discovered with 0.1 AU beams around G-type stars older than $5 \cdot 10^9$ yr.
- In case of the Jupiter-like planet detected around the M2V star Lalande 21185 a linear dimension of 1 AU corresponds to a beam size of $0.4''$. The data deduced for the planet (0.9 Jupiter masses, 0.35 to 1.35 Jupiter radii, 2 AU distance from star, 5.8 years orbital period) would allow an observation of a possible CO_2 band with a relativly large beam size.

Acknowledgements. We thank the unknown referee for the suggestions.

References

André, P., 1994, Disk-like structures around young stars. In: Ferlet, R., Vidal-Madjar, A. (eds.), Circumstellar dust disks and planet formation. Editions Frontieres, p. 115

Artymowicz, P., Burrows, C., Paresce, F., 1989, ApJ **337**, 494

Artymowicz, P., 1994, Modelling and understanding the dust around Beta Pictoris. In: Ferlet, R., Vidal-Madjar, A. (eds.), Circumstellar dust disks and planet formation. Editions Frontieres, p. 47

Burke, B. F. (ed.), 1992, Toward Other Planetary Systems (TOPS), A Report by the Solar System Exploration Division, NASA print, Fig. 4.3, p. 78

Burke, B. F., Rahe, J. H., Roettger, E. E., 1994, AP&SS **212**, 1

Dorschner, J.,Begemann, B., Henning, Th., Jäger, C., Mutschke, H., 1995, A&A **300**, 503

Doyle, L. R., Deeg, H. -J., Martin, E., Jenkins, J. M., Schneider, J., Chevreton, M., Lee, W. -B., Kim, H. -I., Ninkov, Z., Blue, J. E., Stone, R., Toublanc, D., Paleologou, E., Papamastorakis, J., Kozhevnikov, V. P., Zakhavova, P. E., Doyle, M., 1996 BAAS **28**, 1202

Duncan, M., Quinn, Th., Tremaine, S., 1989, Icarus **82**, 402

Fischer, O., Henning, Th., Yorke, H., 1994, A&A **284**, 187

Fischer, O., 1995, Polarization by Circumstellar dust – Modelling and Interpretation of Polarization Maps. In: Reviews in Modern Astronomy, Vol. 7, 1995, p. 103

Holman, M. J., Wisdon, J., 1993, AJ **105**, 1987

Hudgins, D. M., Sandford, S. A., Allamandola, L. J., Tielens, G. G. M., 1993, ApJSS **86**, 713

Knacke, R. F., Fajardo-Acosta, S. B., Telesco, C. M., Hackwell, J. A., Lynch, D. K., Russell, R. W., 1993, ApJ **418**, 440

Lagrange-Henri, A. M., Beust, H., Vidal-Madjar, A., Ferlet, A., 1989, A&A **215**, L5

Lee, H. M., Draine, B. T., 1985, ApJ **290**, 211

Leinert, Ch., Grün, E., 1990, Interplanetary dust. In: Schwenn, R., Marsch, E. (eds.), Physics of the inner heliosphere I, p. 236

Mayor, M., Queloz, D., 1995, Nature **378**, 355

Sandford, S. A., 1988. In: Bailey, M. E. & Williams, D. A. (eds.), Dust in the Universe. Cambridge University Press, Cambridge, p. 193

Schneider, J., 1996a, Overview of detection methods. In: Doyle, L. (ed.), Circumstellar Habitable Zones, Proceedings of the First International Conference on Habitable Zones. Travis House Publications, p. 239

Schneider, J., 1996b Strategies for the Search of Life. In: Chela-Flores & Raulin (eds.), Chemical evolution: physics of the evolution of life. Kluwer, p. 73

Shakura, N. I., Sunyaev, R. A., 1973, A&A **24**, 337

Walker, G., 1996, Nature **382**, 23

Wolszczan, A., Frail, D. A., 1992, Nature **355**, 145

This article was processed by the author using Springer-Verlag LaTeX A&A style file *L-AA* version 3.